HHS Public Access

Author manuscript

Mol Psychiatry. Author manuscript; available in PMC 2023 August 01.

Published in final edited form as:

Mol Psychiatry. 2023 February ; 28(2): 780–791. doi:10.1038/s41380-022-01833-y.

WHOLE-BRAIN WHITE MATTER ABNORMALITIES IN HUMAN COCAINE AND HEROIN USE DISORDERS: ASSOCIATION WITH CRAVING, RECENCY, AND CUMULATIVE USE

Pierre-Olivier Gaudreault, PhD[1], **Sarah G. King, BSc**[1], **Pias Malaker, MSc**[1], **Nelly Alia-Klein, PhD**[1], **Rita Z. Goldstein, PhD**[*,1]

[1]Psychiatry and Neuroscience Departments, Icahn School of Medicine at Mount Sinai, New York City, NY, USA

Abstract

Neuroimaging studies in substance use disorder have shown widespread impairments in white matter (WM) microstructure suggesting demyelination and axonal damage. However, substantially fewer studies explored the generalized vs. the acute and/or specific drug effects on WM. Our study assessed whole-brain WM integrity in three subgroups of individuals addicted to drugs, encompassing those with cocaine (CUD) or heroin (HUD) use disorder, compared to healthy controls (CTL).

Diffusion MRI was acquired in 58 CTL, 28 current cocaine users/CUD+, 32 abstinent cocaine users/CUD−, and 30 individuals with HUD (urine was positive for cocaine in CUD+ and opiates used for treatment in the HUD). Tract-Based Spatial Statistics allowed voxelwise analyses of diffusion metrics [fractional anisotropy (FA), mean diffusivity (MD), radial diffusivity (RD), and axial diffusivity (AD)]. Permutation statistics (p-corrected<.05) were used for between-group t-tests.

Compared to CTL, all individuals with addiction showed widespread decreases in FA, and increases in MD, RD, and AD (19-57% of WM skeleton, p<.05). The HUD group showed the most impairments, followed by the CUD+, with only minor FA reductions in CUD− (<.2% of WM skeleton, p=.05). Longer periods of regular use were associated with decreased FA and AD, and higher subjective craving was associated with increased MD, RD, and AD, across all individuals with drug addiction (p<.05).

These findings demonstrate extensive WM impairments in individuals with drug addiction characterized by decreased anisotropy and increased diffusivity, thought to reflect demyelination and lower axonal packing. Extensive abnormalities in both groups with positive urine status

[*]**Corresponding author:** Rita Z. Goldstein, PhD, Mount Sinai Professor in Neuroimaging of Addiction, Department of Psychiatry (primary) and Department of Neuroscience (secondary), Chief, Neuropsychoimaging of Addiction and Related Conditions (NARC) Research Program, Icahn School of Medicine, Gustave L. Levy Place, Box 1230, New York, NY 10029, Tel: 212-659-8886, rita.goldstein@mssm.edu.

Contributions

Study design: POG, NAK, RZG. Data management: PM. Data analysis: POG, SGK. Initial Manuscript writing: POG. Manuscript review: POG, SGK, PM, NAK, RZG.

Supplementary information is available at MP's website.

Disclosures

The authors report no biomedical financial interests or potential conflicts of interest.

(CUD+ and HUD), and correlations with craving, suggest greater WM impairments with more recent use. Results in CUD−, and correlations with regular use, further imply cumulative and/or persistent WM damage.

Introduction

Drug addiction is a complex and chronic brain disorder that encompasses periods of intoxication and compulsive drug-seeking usually followed by withdrawal and drug-related cravings that repeat despite adverse consequences [1]. Functional neuroimaging studies have consistently revealed cognitive and emotional impairments in individuals with substance use disorders (SUD), associated with the recruitment of multiple large-scale brain networks (including reward, habit, salience, executive, memory, and self-directed networks) during drug-related processing, and reduced responses in these networks during non-drug-related processing [see [2] for an extensive review]. The neurobiological correlates of these dysfunctions implicate gray and white matter deficits, especially in the prefrontal cortex (PFC) but also in tracts projecting to and from the PFC [see [3] for a recent review].

Using diffusion tensor imaging (DTI), the current state-or-the-art technique to quantitatively assess the brain's white matter (WM) microarchitecture, several studies reported impairments in nicotine, alcohol, cannabis, methamphetamine, cocaine, and opiate use disorders as recently reported in a review [4], a meta-analysis [5], and a mega-analysis [6]. In individuals with addiction to cocaine and heroin, the two illicit drugs considered to cause the most dependence and harm [7], WM abnormalities have been observed in all major WM tracts, especially in projections to and from PFC regions. These included decreased fractional anisotropy (FA) and increased mean diffusivity (MD) in cocaine addiction [8–11], suggestive of myelin damage. Together with reduced FA, higher radial (RD) and axial diffusivities (AD) further suggest alterations in axonal integrity as observed in individuals with opiate including heroin addiction [12–16]. Furthermore, impaired WM microstructure in the tapetum in cocaine users [10], and more globally in the frontal WM of heroin users [14, 17], was correlated with longer duration of drug use, suggesting the impact of chronicity of use.

However, there has been relatively less emphasis on studying the impact of addiction generally vs. acute/specific effects of a particular drug on these WM microstructural alterations. To the best of our knowledge, only one study directly compared individuals addicted to stimulants or opiates, showing frontal WM hyperintensities in T2-weighted MRI images in both groups compared to healthy subjects [18]. In this prior study, compared to opiate addiction, cocaine addiction was associated with both higher prevalence (including global, deep brain, and insular hyperintensities) and severity of these abnormalities, which may reflect the more severe cardiovascular effects associated with cocaine use [19].

The objective of the current whole-brain diffusion MRI study was to compare healthy controls (CTL) and individuals with SUD, including two cohorts of individuals with cocaine use disorder (CUD) or heroin use disorder (HUD). We further explored individual differences within the CUD group by dividing it to two subgroups [abstinent = negative urine toxicology for cocaine (CUD−) vs. current users = positive urine toxicology for

cocaine (CUD+)] to test the potential impact of acute drug effects. Based on prior studies, we expected to observe WM abnormalities, characterized by reduced FA and increased MD, RD, and AD, across all individuals with SUD when compared to CTL. Given the mean length of abstinence in the CUD− group (>1 year), and in accordance with our previous study [20], we expected less pronounced WM abnormalities in this subgroup as compared with the CUD+ group. Finally, a direct comparison between the HUD group and both CUD subgroups was intended to further our understanding of the role of general addiction (to cocaine or heroin) vs. specific drug effects on WM. Given the positive urine status of the HUD group [on medically-assisted treatment (MAT) and hence putatively more similar to the CUD+] but also their time since last heroin use (>6 months and hence putatively more similar to the CUD−), directionality of these effects was exploratory.

Methods and Materials

Participants

Ninety individuals with SUD (60 with CUD and 30 with HUD undergoing MAT) and 58 CTL were recruited as part of two research protocols [data for 27 CTL and 25 CUD was previously reported [6], and a subsample of 28 CTL, 15 CUD−, 16 CUD+, and 24 HUD participants was also included in a separate analysis where we employed methods suitable for modeling precise structural connections that cannot be otherwise analyzed using whole-brain methods, which included both T1 and T2-weighted scans in addition to diffusion weighted imaging and a fiber orientation diffusion function pipeline to assess specific PFC-habenula WM fiber bundles [21]]. Although a major difference between the CUD and HUD groups was in their inpatient status (true only for the latter), all individuals with SUD were recruited from advertisements and flyers as well as from educational talks provided at collaborating substance abuse treatment institutes in the New York metropolitan area (e.g., Samaritan Daytop Village, NY). Healthy controls were recruited from the same communities for matching purposes. The CUD group included 32 abstinent users (average abstinence by self-report: 18 months) and 28 current users (average abstinence: 3 days), as further confirmed by objective urine screens. All participants provided written informed consent and study procedures were approved by the Icahn School of Medicine at Mount Sinai's institutional review board. The same highly trained study team supervised by senior clinical psychologists conducted all subject evaluations that included both objective and subjective, categorical and continuous, measures/tools encompassing the Structured Clinical Interview for the *Diagnostic and Statistical Manual of Mental Disorders, fourth edition* [22] (used for CTL and the CUD) or the Mini International Neuropsychiatric Interview [23] (used for the HUD), and the Addiction Severity Index [24] (used for all SUD). The CUD participants met criteria for current cocaine dependence (n=32), abuse (n=3), or dependence in remission (n=25). All HUD participants met criteria for SUD with heroin being their primary drug of choice. Within the CUD sample, eight also met criteria for HUD, and within the HUD sample, nine also met criteria for CUD; however, these individuals' primary drug of abuse was determined to be congruent with their assignment to their respective groups. The route of drug administration included smoking (41 CUD/3 HUD), intra-nasal (18 CUD/11 HUD), intravenous (1 CUD/15 HUD), and oral (1 HUD). Other comorbidities included alcohol use disorder (22 CUD, 3 HUD), marijuana use disorder (9 CUD, 1 HUD), amphetamine use

disorder (1 CUD, 2 HUD), polysubstance use disorder (3 CUD, 2 HUD), and post-traumatic stress disorder (1 CUD, 1 HUD). All SUD comorbidities were in partial or sustained remission at the time of study. For the CUD or HUD groups, respectively, symptoms of withdrawal were assessed with the Cocaine Selective Severity Assessment [25] or the Subjective Opiate Withdrawal Scale [26]; and symptoms of craving were assessed with the 5-item Cocaine Craving Questionnaire [27] or the Heroin Craving Questionnaire – Short form-14 [28] on the day of the scan. These scores were range-corrected to a common scale for group comparisons. Dependence severity was assessed with the Severity of Dependence Scale [29] and the Fagerström Test for Nicotine Dependence [30] was used to measure nicotine dependence in all subjects. Nicotine use was also tested objectively with a carbon monoxide breath test. Recency of drug use was assessed in all participants objectively with a urine toxicology test and a breathalyzer test for alcohol use and by self-reports on each study day. Urine was positive for cocaine for the CUD+; it was negative for the CUD−. With the exception of one participant, all individuals with HUD were urine negative for heroin, but all tested positive for other opiates [those used for MAT: methadone n=25 (106.5±62.0mg, 1 missing), buprenorphine/naloxone n=5 (14.7±8.3mg, 2 missing)]. Exclusion criteria were: 1) present or past history of DSM-IV diagnosis of psychotic disorder or neurodevelopmental disorder; 2) history of head trauma with loss of consciousness (>30 min); 3) history of neurological disorders including seizures; 4) current use of any medication (with the exception of MAT in the HUD) that may affect neurological functions; 5) current medical illness and/or evident infection including cardiovascular disease (e.g., high blood pressure), as well as metabolic, endocrinological, oncological or autoimmune diseases, and infectious diseases common in individuals with SUD including Hepatitis B and C or HIV/AIDS; 6) MRI contraindications including any metallic implants, pacemaker device, or pregnancy. We did not exclude SUD subjects for history of other drug addiction (e.g., alcohol, marijuana, stimulants/opiates) or other psychiatric disorders with high rates of comorbidity with drug addiction (e.g., depression, post-traumatic stress disorder); 7) a positive breathalyzer test for alcohol; and 8) MRI quality assurance, including the presence of incidental findings in the WM as indicated by a radiologist, bad diffusion data, or an MRI session that did not include a diffusion sequence (9 CUD/1 HUD/7 CTL). The CTL subjects were recruited and assessed by the same study team with the same tools (with the exception of the withdrawal, craving, and severity of dependence scales) meeting the same exclusion criteria as the SUD with the exception for a positive urine screen for any psychoactive drugs or history of any SUD that were exclusionary for this group.

Behavioral Assessment

All subjects were assessed for demographic characteristics and estimated verbal (with the reading subtest of the Wide Range Achievement Test-3 [31]) and non-verbal IQ (with the Matrix Reasoning subtest of the Wechsler Abbreviated Scale of intelligence [32]). In addition, depression was evaluated with the Beck Depression Inventory (BDI) [33] and anxiety symptoms were measures with the Beck Anxiety Inventory (BAI) [34]. Handedness was assessed with the modified Edinburgh Handedness Inventory [35] (See Table 1).

MRI Acquisition

MRI acquisition was performed using a Siemens 3.0 Tesla Skyra scanner (Siemens Healthineers AG, Erlangen, Germany) with a 32-channel head coil. Diffusion MRI data were acquired using an echo-planar sequence with opposite phase encoding along the left-right axis, monopolar diffusion encoding with 128 diffusion-weighted images (2×64 for each encoding phase) at single shell maximum b=1500 s/mm^2, 13 reference images at b=0 s/mm^2, field of view (FOV) = 882×1044 mm, 1.8 mm isometric voxel size, repetition time (TR) = 3650 ms, echo time (TE) = 87 ms, bandwidth = 1485 Hz/px, and 80° flip angle, multiband = 3, no in-plane acceleration. A structural T1-weighted scan was acquired using an MPRAGE sequence, sagittal orientation [FOV = 256×256×179 mm^3; 0.8 mm isotropic resolution; TR 2400 ms; TE 2.07 ms; inversion time 1000 ms; flip angle 8° with binomial (1, −1) fat saturation; bandwidth 240 Hz/pixel; 7.6 ms echo spacing, and in-plane acceleration (GRAPPA) factor of 2] and was used for intracranial volume (ICV) estimation.

Diffusion Tensor Imaging (DTI) Processing

Diffusion MRI images were preprocessed with the MRtrix3 [36] and FMRIB Software Library (FSL 6.0) [37] toolboxes. First, the images were denoised using Marchenko-Pastur PCA [38]. Then, using MRtrix3's "*dwifslpreproc*" that integrates FSL's "*eddy*" and "*topup*" commands, images were preprocessed and corrected for eddy current-induced distortions, motion artifacts and susceptibility-induced distortions [39]. For quality assurance, we made sure that the proportion of outlier slices in each scan (CTL = .127 ± .193%, CUD− = .325 ± .578%, CUD+ = .431 ± .715%, HUD = .561 ± .604%) was below the reference threshold of 10% [40]. We also extracted the amount of absolute displacement (in mm) that was corrected during the preprocessing step, which showed a sub-voxel averaged motion correction by the "eddy" and "topup" commands and no group differences that reached nominal significance level (Table 1). All scans were visually inspected to detect major data abnormalities. Diffusion tensors were fitted to each voxel and quantitative maps of diffusion metrics (FA, MD, RD, and AD) were derived from the three orthogonal eigenvectors extracted from each tensor. Fractional Anisotropy reflects the coherence of water diffusion along a specific orientation and MD represents the magnitude of diffusion whereas RD and AD represent the diffusion across the axonal membrane and parallel to the orientation of the axon, respectively. Tract-based spatial statistics (TBSS) was then used to perform whole-brain voxelwise analyses across all participants by, first, aligning and registering individual FA maps to a standard MNI152 template using non-linear registration to create a WM skeleton from the averaged maximal FA [41]. Individual DTI maps (of all four metrics) were then projected back onto this skeleton to perform voxelwise group-level statistical tests. Results are presented as percentages of the 98,859 voxels comprising the WM skeleton, which represents the extent of the significant voxels throughout the brain.

Statistical Analyses

All variables in Table 1 (demographic, neuropsychological, and drug use variables) were compared between CTL and all individuals with SUD (CUD−, CUD+, and HUD), or only within SUD as appropriate, using one-way ANOVAs for continuous variables and Chi-square (χ^2) tests for categorical variables. Post-hoc analyses included Tukey HSD tests

for F statistics and Bonferroni-corrected adjusted residuals for Chi-square tests. In order to correct for multiple comparisons, p values for group effects were considered significant at $p < .005$ (.05/11 tests) for the demographic and neuropsychological measures, and at $p < .004$ (.05/13 tests) for the drug use variables.

The main set of whole-brain analyses investigated group differences between the CTL and individuals with SUD in the four WM diffusion metrics using a design matrix coding for independent groups t-tests (two contrasts: CTL > SUD and CTL < SUD). For our second and third objectives, specific between-subgroups differences were computed using independent t-statistic contrasts between all group pairs (analogous to testing simple effects in an ANOVA). Significant main effects of group averages were also confirmed using F-tests that yielded similar results. Therefore, since the t-tests were more specific in testing directionality of contrasts (CTL > SUD and CTL < SUD) whereas the F-tests only provide voxels where significant group effect was found, independent of the direction of the difference itself, we do not present the maps of the main effect of group from the F-tests in the main text; instead, we summarized these F-tests results in Supplementary Table 1 and Supplementary Figure 1. All whole-brain WM analyses were carried out with FSL tool "*Randomise*," a general linear model for non-parametric permutation inferences [41] using 10,000 permutations. To account for multiple comparisons, threshold-free cluster enhancement (TFCE) correction, aiming at better discriminating clustered voxels by enhancing areas of signal exhibiting spatial contiguity, was applied for each analysis [42]. A cluster was considered significant when at least 100 contiguous voxels reached the voxelwise threshold of $1\text{-}p > .949$. For our exploratory analyses (aiming at comparing the two CUD subgroups to the HUD group), we reduced the cluster threshold to 15 contiguous significant voxels, and considered anything below our 100 voxels threshold as a trend. Neuroanatomical localization of WM tracts was performed with the FSL "*atlasquery*" toolbox and "*JHU ICBM-DTI-81 White-Matter Labels*" atlas [43], with an average probability of region overlap threshold of 2%.

To control for potential covariates of interest (see Table 1 for variables that differed between the groups), we inspected ICV as well as any demographic, neuropsychological, or drug use variables that differed between groups: age, education, race, verbal IQ, depression, anxiety, nicotine dependence (FTND score), and days of alcohol use in the past 30 days. Although the groups did not differ in gender distribution, this variable was also included because of its known effect on diffusion metrics [44–46] and because it remains unclear whether there is statistical redundancy while correcting for both gender and ICV [47]. For these variables, we performed two sets of preliminary analyses. For the continuous variables, whole-brain correlations were performed with the z-scored variable of interest and independent group analyses (t-tests) were carried out for the categorical variables. Due to the number of comparisons (ten variables and four diffusion metrics), the inclusion of a covariate was determined by a significance threshold of $1\text{-}p > .9988$. None of these analyses reached significance except for age and ICV, which we added to the whole-brain group comparisons. No covariates were added to the exploratory correlation analyses.

We used a similar approach for the drug use variables that showed significant differences between the SUD subgroups (days of drug of choice use in the previous 30 days, years

of regular use of the drug of choice, severity of dependence, and subjective cravings). Whole-brain voxelwise correlations were performed using z-scored for these four drug use measures across all SUD participants; for completeness, we similarly inspected abstinence (that did not show a significant group effect after family-wise corrections). The magnitude of the correlations (r values) was estimated by averaging the extracted WM metrics from significant voxels and computing the correlations using IBM SPSS statistics version 25 (IBM Corp, Armonk, NY). Because of the exploratory nature of these correlational analyses, significance was considered with a voxelwise threshold of 1-p > .949 in at least 100 contiguous voxels for whole-brain voxelwise analyses and a threshold of $p < .05$ for analyses on extracted WM metrics values. To further control the potential effect of alcohol use in the past 30 days and severity of nicotine dependence, we performed hierarchical regressions whereby these two measures were entered first, followed in the second step by adding the drug use variables that were significantly associated with the DTI metrics (which were the dependent measures in these regressions).

Results

Demographic, neuropsychological, and drug use variables

The groups differed on age, education, verbal IQ, depression and anxiety such that CTL and HUD subjects were younger than both CUD groups ($p < .01$), CTL had more years of education compared to all SUD groups ($p < .01$) and higher verbal IQ compared to the CUD+ ($p < .05$) and HUD subgroups ($p < .01$), and the HUD group reported higher depression ($p < .05$) and anxiety symptoms ($p < .01$) compared to the other three groups (Table 1). Groups also differed on race, where the HUD group was comprised of significantly more White participants ($p < .004$) than the other groups. For the drug use variables, groups differed on smoking status where the CTL group was comprised of significantly more individuals who never smoked ($p < .00001$), all SUD groups included more current smokers than the control group ($p < .003$), and the HUD and CUD+ groups included more current cigarette smokers than the CUD− group. The severity of nicotine dependence was significantly higher in the HUD and CUD− groups ($p < .05$). The SUD groups also differed on days of alcohol use during past 30 days ($p < .001$) where the CUD+ group drank on more days than the CUD− ($p < 0.05$) and HUD groups ($p < 0.0001$). Significant between-group differences in the primary drug of use (cocaine or heroin) were found for years of regular use, days of drug use during the previous 30 days [higher in the CUD+ group compared to CUD− and HUD ($p < .01$)], severity of dependence [higher in the HUD group compared to both CUD groups ($p < .001$)] and craving [higher in the HUD and CUD+ compared to the CUD− ($p < .01$)]. It is important to note that the individuals with HUD were inpatients living in a drug rehabilitation facility at the time of the study, potentially contributing to the high drug cravings despite being stabilized on MAT.

Whole-brain white matter abnormalities in individuals with substance use disorder

The significant whole-brain WM differences between the CTL subjects and individuals with SUD are presented in Figure 1 with specific clustered results and localizations summarized in Supplementary Table 2 (Supplementary Table 3 also summarizes the percentages of significant voxel across the WM skeleton for each contrast/diffusion metric). Individuals

with SUD showed significantly lower FA (43.7%, .949 < 1-p < .999) as well as higher MD (56.8%, .949 < 1-p < .993), RD (56.6%, .949 < 1-p < .998), and AD (18.8%, .949 < 1-p < .989) in all major WM tracts when compared to CTL. More specifically, individuals with SUD showed lower FA in commissural and projection fibers. Mean diffusivity and RD were significantly higher in the same commissural tracts and projection fibers. Mean diffusivity was also specifically increased in brainstem WM fibers. Finally, individuals with SUD showed higher AD in bilateral projection and in multiple association fibers. We also assessed the putative impact of the absolute motion correction on FA, since it is the most vulnerable diffusion metric to the inclusion of poorly corrected images [48]. No effect of absolute displacement was found ($F(1,145) = .12$, $p = .733$), and the group effects we reported for FA remained significant after inclusion as covariate of the absolute motion correction ($F(3,145) = 16.5$, $p < .001$).

Group-specific whole-brain abnormalities in abstinent and current cocaine users

For this section and the one below (comparisons with HUD), all significant contrasts are presented in Figure 2 for the FA and MD results and in Figure 3 for the AD and RD results. Clustered results with corresponding atlas location are also presented in Table 2 (see also Supplementary Table 3). Control subjects showed higher FA than the CUD− group in a small cluster located in left projection fibers (.17%, .949 < 1-p < .951). No other diffusion metric showed significant effect for this contrast. Global WM abnormalities were also found when comparing CTL to the CUD+ group encompassing decreased FA (11.9%, .949 < 1-p < .989), as well as increased MD (65.5%, .949 < 1-p < .998), RD (57.9%, 0.949 < 1-p < 0.998), and AD (28.9%, .949 < 1-p < .995). More specifically, decreased FA was found in commissural, projection, and in association fibers. The other diffusion metrics were increased in a significant portion of the WM skeleton similarly encompassing commissural, projection, and association fibers. Finally, when directly compared with CUD−, the CUD+ group showed higher MD (46.1%, .949 < 1-p < .986), RD (20.9%, .949 < 1-p < .973), and AD (40.1%, .949 < 1-p < .997) in a substantial part of the WM skeleton including commissural fibers, most projection fibers as well as association fibers.

Group-specific whole-brain abnormalities in cocaine and heroin use disorder

We also explored whether the whole-brain WM abnormalities observed in the CUD groups were generalizable to individuals with HUD. In addition to Figures 2–3, clustered results are presented in Table 2 (see also Supplementary Table 3). When compared to CTL, individuals with HUD showed a general decrease in FA and increased MD, RD and AD (respectively 45.1%, 56.6%, 58.9%, and 26.8%, all .949 < 1-p < .999). Specifically, FA changes were found in commissural and projection fibers, while the MD, RD, and AD effects were similarly found in commissural and projections fibers, but also in association fibers (for MD and AD) and fibers emanating from the brainstem (for MD and RD). Similar effects were found when comparing individuals with HUD to CUD− [decreased FA (15.0%, .949 < 1-p < .985) and increased MD (40.0%, .949 < 1-p < .991), RD (35.8%, .949 < 1-p < .990), and AD (24.6%, .949 < 1-p < .999)]. This decreased FA was found in commissural, projection, and association fibers. Increased MD, RD, and AD were also found in commissural, projection, association fibers (for MD and AD only), as well as in fibers connecting the brainstem (for RD only). Interestingly, a trend for a significant reduction in FA was also observed when

comparing individuals with HUD to those with CUD+ in part of the splenium of the corpus callosum (28 voxels, .03%, 1-p = .949).

Correlations between drug use variables and white matter diffusion metrics

Across all SUD, whole-brain voxelwise correlation analyses showed significant negative correlations between regular use and FA (.67%, .949 < 1-p < .974, extracted cluster: r = .49, p < .00001) and AD (5.1%, .949 < 1-p < .965, extracted cluster: r = .42, p < .0001) where more years of regular use was associated with decreased FA and AD (Figure 4A). Significant positive correlations between subjective craving scores and WM diffusivities were also found (Figure 4B) showing that higher baseline craving was associated with higher MD (48.1%, .949 < 1-p < .989, extracted cluster: r = .34, p < .01), RD (11.2%, .949 < 1-p < .971, extracted cluster: r = .42, p < .0001), and AD (33.5%, .949 < 1-p < .992, extracted cluster: r = .46, p < .00001). Adding alcohol use in the past 30 days and the severity of nicotine dependence as the first step of a hierarchical regression model to account for the neurotoxic effects of alcohol and nicotine use, all above correlations remained significant (See Supplementary Table 4).

Discussion

The goal of this study was to assess WM abnormalities in three groups of individuals addicted to drugs to explore the generalized vs. acute/specific drug effects using highly reliable acquisition parameters and analytical specificity. Our study replicated previous reports in the literature, consistent with an emerging consensus supporting widespread WM microstructure abnormalities, characterized by decreased FA, and increased MD, RD, and AD, across all major WM tracts, generalizable across individuals with SUD. Our results showed that between 19% and 57% of the WM skeleton was affected. In addition to the comparison between psychostimulants and opiates for generalizability purposes, we also investigated the contribution of recency of drug use (in the CUD+ and CUD−, who used cocaine on average within three days or 18 months of the study, respectively, and in the HUD, all currently using opiates as part of MAT). Results showed more severity in heroin vs. cocaine users (most severity in the HUD vs. CUD) and a more detrimental effect of more recent drug use (most severity in the HUD and CUD+ vs. CUD−). Among all individuals with SUD, longer periods of regular use were associated with decreased FA and AD and higher subjective craving was associated with increased MD, RD, and AD.

Individuals with HUD showed the most pronounced impairments followed by the CUD+, with the CUD− showing the least impairment (different from CTL only in a small cluster located in projection fibers of the internal capsule). Specifically, the HUD group showed more widespread FA impairments than CUD+ (45.1% vs. 11.9% of WM skeleton); a direct comparison revealed a significant difference in the splenium of the corpus callosum (lower FA in HUD vs. CUD+). This pattern of results, and correlations with craving (the higher the craving, the higher the MD, RD, and AD across all SUD), suggest the detrimental effects of acute/recent drug use on the brain (indicated by a positive drug urine status for both CUD+ and HUD groups), with potentially more specificity and severity of the effect for opiates vs. stimulants. The severity of dependence (highest in the HUD group, all inpatients on

MAT) and more years of regular use (highest in the CUD+) may have also contributed to the pattern of results observed in our study. Indeed, across all individuals with SUD, more years of regular use was associated with a reduction of FA and AD. Similar associations between WM abnormalities with duration of regular use were previously reported in the tapetum in CUD [10] and in frontal pathways in HUD [14, 17] [and in the inferior frontal gyrus in alcohol use disorder [49]]. Of note are the seemingly contradictory results for AD (i.e., decrease with years of use and increase with craving). Upon closer inspection, there was minimal overlap (<3% of the WM skeleton) of the maximal peak, with a specific subcortical involvement for the association with regular use and a more widespread cortical effect for the association with craving. Taken together, these results support the detrimental effects of both chronicity and recency of use of both drug types.

The white matter abnormalities across both substance types documented in our study are consistent with previous diffusion MRI findings in addiction to cocaine [5, 6, 8–11] and heroin [12–17] as well as heavy use of other types of drugs [4, 49–55] (encompassing alcohol, nicotine and marijuana) when compared to demographically matched CTL groups. However, our results highlight a more extensive pattern of WM abnormalities than previously reported, encompassing fronto-striatal and fronto-temporal projections, involved in the regulation of learning and memory, executive control, and reward-driven behaviors, but also centro-parietal projections and association WM tracts (such as the corona radiata, the posterior thalamic radiation, and the superior longitudinal fasciculus), which constitute major intrahemispheric connections. The current findings therefore support, and extend, previous results showing widespread, seemingly non-specific changes in WM tracts across multiple groups of individuals with SUD transcending numerous differences between the various drug classes. The contribution of these broad WM results to specific cognitive (e.g., inhibitory control), emotional (e.g., cue reactivity), functional, and anatomical deficits that characterize SUD remains to be studied. In general, the pattern observed in the SUD subjects (reduced FA concomitantly with increases in MD and RD but also AD) is indicative of WM impairment, as has been shown in brain disorders with both normal-appearing or abnormal WM including multiple sclerosis, stroke, dementia, and schizophrenia [56–58]. These changes in WM have been associated with neurobiological correlates of demyelination, decreased axonal packing [59, 60], axonal degeneration, axonal loss [61, 62], neurofilament damage and WM fiber atrophy, and increased extracellular water content [60, 63, 64], although these effects remain to be validated by preclinical/ex vivo studies. Although the direct measurement of these physiological processes on a microscopic scale is not possible with DTI, in a rodent model of cocaine addiction reduced white matter FA and increased RD were specifically colocalized with myelin damage and destabilized neurite outgrowth in the internal capsule and the corpus callosum [65], supporting our analysis of all four DTI metrics (FA, MD, RD, and AD), which captures specific and complementary changes in tissue microstructure [66]. Nevertheless, because of the redundancy in the calculation of some of these measures [67], new analysis frameworks aiming at reducing the dimensionality of diffusion data might help clarify the neurobiological underpinnings of WM impairments [68].

Importantly, our results also confirmed the generalization of these WM impairments across two different classes of drugs of abuse (stimulants and opiates) that are known for their

neurotoxic effects associated with neuroinflammatory brain responses [69, 70], which may in turn precipitate myelin degradation [71, 72]. Shared neurobiological mechanisms contributing to these widespread WM insults may involve neuroplastic processes like the modulating effect exerted by the dopaminergic system on axonal myelination throughout the brain [73–75] as stimulants directly bind to the dopamine transporters [76] whereas opiates act indirectly on the dopaminergic system by activating the mu opioid receptors on GABAergic interneurons in the ventral tegmental area [77]. Oxidative stress responses, down-regulation of myelin-related protein expression, mitochondrial dysfunction, and/or neuronal apoptosis could also serve as other potential neurophysiological mechanisms underlying the WM abnormalities in these two drug classes [11, 78–81]. Other processes may also include reduced efficiency of glial cells in regulating glutamate homeostasis and blood-brain barrier dysfunctions exposing the brain to toxins [70, 82]. Axonal and myelin degeneration could also result from vascular effects of both classes of drugs through stimulant-induced vasoconstriction, increasing the risk of hypoperfusion [83, 84], and/or through opiate-related ischemic lesions and perfusion deficits, potentially induced by respiratory suppression, altered consciousness, overdoses, or other vascular conditions (e.g., vasculitis and rhabdomyolysis) that are often observed in heroin/opiate users [85, 86].

Beyond the precise neurobiological mechanisms, the importance of these results is in their potential for outcome prediction: in other studies of individuals with HUD undergoing MAT, these WM abnormalities were observed in those who relapsed (positive urine status for both methadone and heroin) as compared to those who abstained (positive urine status for methadone but not heroin); further recovery was associated with less severe impairments in individuals with HUD in prolonged abstinence (negative urine status) [13, 87, 88]. Positive correlations between long-term abstinence and WM integrity in the ventromedial PFC/orbitofrontal cortex in individuals with CUD and in frontal WM in opiate/heroin addiction [8, 12, 17] also support this possibility. Our own results in the CUD-similarly suggest that longer abstinence length durations (and/or less chronicity of use) could potentially contribute to WM recovery as remains to be tested in longitudinal studies. Nevertheless, it is important to consider that some of the WM microstructure impairments may be persistent, as suggested by the significant FA reductions in this group compared to the CTL group, consistent with similar results in the internal capsule of individuals with methamphetamine use disorder [89].

Several limitations are important to consider. First, the groups showed significant differences in age, education, race, verbal IQ, depression, anxiety, severity of nicotine dependence and alcohol use in the past 30 days. While these variables did not correlate with our dependent variables and thus could not have substantially contributed to the results, larger, more closely-matched samples may better tease apart the potential contributions of these individual differences. Longitudinal within-subject studies are also needed to ascertain the impact of abstinence, and other time-varying metrics, on our results. In addition to the three SUD groups included here, recruiting a group of abstinent heroin users (inclusive of MAT, HUD−) as well as a group of current heroin users (HUD+) could help clarify the distinction between the acute effect of the drug and the specificity of impairments to stimulants vs. opiates. Future studies should also include a group of polysubstance users, as increases in demyelination in PFC regions (i.e., increased RD) were previously

associated with the number of substances used [90], potentially indicative of a dose effect. Another limitation lies in the underrepresentation of women in our sample, which should be specifically addressed in upcoming studies to understand the possible gender-related differences in WM microstructure effects, as suggested in a population study of WM integrity [91]. Finally, although TBSS provides a voxelwise whole-brain measure of WM differences between groups, the DTI model on which it relies often lacks specificity in areas where the architecture of the WM fibers is more complex (e.g., multiple population of fibers, crossing or kissing fibers) [67]. Therefore, future studies should also aim at using advanced diffusion methodology known to be more robust in identifying complete WM fiber bundles (i.e., orientation distribution function) to model specific components of the salience/reward, executive control, and learning networks, and explore associations between the integrity of specific WM tracts and impaired behavioral and neurocognitive functioning in SUD.

In conclusion, we report whole-brain widespread WM abnormalities across individuals with SUD as driven by HUD on MAT and CUD+, and correlations with craving that together suggest the impact of the acute effects of both opiates and stimulants on WM integrity, with results also pointing to the specificity of this effect (i.e., reduced FA for HUD>CUD+ in the splenium of the corpus callosum). The lower extent of impairment in the CUD− corroborates previous findings of brain recovery with abstinence/less current use but the persistence of these impairments, and correlations with years of regular use across all SUD, also suggest the detrimental effect of chronicity of drug use on WM integrity in drug addiction.

Supplementary Material

Refer to Web version on PubMed Central for supplementary material.

Acknowledgments

This work was supported by the National Institute on Drug Abuse (Goldstein, 1R01DA048301-01A1), the National Center for Complementary and Integrative Health (Goldstein, 1R01AT010627-01), and the Canadian Institutes of Health Research (Gaudreault, postdoctoral research fellowship).

References

1. Volkow ND, Fowler JS. Addiction, a Disease of Compulsion and Drive: Involvement of the Orbitofrontal Cortex. Cerebral Cortex. 2000;10:318–325. [PubMed: 10731226]
2. Zilverstand A, Huang AS, Alia-Klein N, Goldstein RZ. Neuroimaging Impaired Response Inhibition and Salience Attribution in Human Drug Addiction: A Systematic Review. Neuron. 2018;98:886–903. [PubMed: 29879391]
3. Ceceli AO, Bradberry CW, Goldstein RZ. The neurobiology of drug addiction: cross-species insights into the dysfunction and recovery of the prefrontal cortex. Neuropsychopharmacol. 2022;47:276–291.
4. Hampton WH, Hanik IM, Olson IR. Substance abuse and white matter: Findings, limitations, and future of diffusion tensor imaging research. Drug and Alcohol Dependence. 2019;197:288–298. [PubMed: 30875650]
5. Suchting R, Beard CL, Schmitz JM, Soder HE, Yoon JH, Hasan KM, et al. A meta-analysis of tract-based spatial statistics studies examining white matter integrity in cocaine use disorder. Addiction Biology. 2020;26.
6. Ottino-González J, Uhlmann A, Hahn S, Cao Z, Cupertino RB, Schwab N, et al. White matter microstructure differences in individuals with dependence on cocaine, methamphetamine, and

nicotine: Findings from the ENIGMA-Addiction working group. Drug and Alcohol Dependence. 2022;230:109185. [PubMed: 34861493]

7. Nutt D, King LA, Saulsbury W, Blakemore C. Development of a rational scale to assess the harm of drugs of potential misuse. The Lancet. 2007;369:1047–1053.
8. He Q, Li D, Turel O, Bechara A, Hser Y-I. White matter integrity alternations associated with cocaine dependence and long-term abstinence: Preliminary findings. Behavioural Brain Research. 2020;379:112388. [PubMed: 31783090]
9. Romero MJ, Asensio S, Palau C, Sanchez A, Romero FJ. Cocaine addiction: Diffusion tensor imaging study of the inferior frontal and anterior cingulate white matter. Psychiatry Research: Neuroimaging. 2010;181:57–63.
10. van Son D, Wiers RW, Catena A, Perez-Garcia M, Verdejo-García A. White matter disruptions in male cocaine polysubstance users: Associations with severity of drug use and duration of abstinence. Drug and Alcohol Dependence. 2016;168:247–254. [PubMed: 27736678]
11. Tondo LP, Viola TW, Fries GR, Kluwe-Schiavon B, Rothmann LM, Cupertino R, et al. White matter deficits in cocaine use disorder: convergent evidence from in vivo diffusion tensor imaging and ex vivo proteomic analysis. Transl Psychiatry. 2021;11:252. [PubMed: 33911068]
12. Bora E, Yücel M, Fornito A, Pantelis C, Harrison BJ, Cocchi L, et al. White matter microstructure in opiate addiction. Addiction Biology. 2012;17:141–148. [PubMed: 21070508]
13. Li W, Zhu J, Li Q, Ye J, Chen J, Liu J, et al. Brain white matter integrity in heroin addicts during methadone maintenance treatment is related to relapse propensity. Brain Behav. 2016;6.
14. Liu H, Li L, Hao Y, Cao D, Xu L, Rohrbaugh R, et al. Disrupted White Matter Integrity in Heroin Dependence: A Controlled Study Utilizing Diffusion Tensor Imaging. The American Journal of Drug and Alcohol Abuse. 2007;34:562–575.
15. Li W, Li Q, Zhu J, Qin Y, Zheng Y, Chang H, et al. White matter impairment in chronic heroin dependence: A quantitative DTI study. Brain Research. 2013;1531:58–64. [PubMed: 23895765]
16. Wang X, Yu R, Zhou X, Liao Y, Tang J, Liu T, et al. Reversible brain white matter microstructure changes in heroin addicts: a longitudinal study: Reversible WM heroin addicts. Addiction Biology. 2013;18:727–728. [PubMed: 21762286]
17. Wollman SC, Alhassoon OM, Stern MJ, Hall MG, Rompogren J, Kimmel CL, et al. White matter abnormalities in long-term heroin users: a preliminary neuroimaging meta-analysis. The American Journal of Drug and Alcohol Abuse. 2015;41:133–138. [PubMed: 25664621]
18. Lyoo IK, Streeter CC, Ahn KH, Lee HK, Pollack MH, Silveri MM, et al. White matter hyperintensities in subjects with cocaine and opiate dependence and healthy comparison subjects. Psychiatry Research: Neuroimaging. 2004;131:135–145.
19. Neiman J, Haapaniemi HM, Hillbom M. Neurological complications of drug abuse: pathophysiological mechanisms. European Journal of Neurology. 2000;7:595–606. [PubMed: 11136345]
20. Parvaz MA, Moeller SJ, d'Oleire Uquillas F, Pflumm A, Maloney T, Alia-Klein N, et al. Prefrontal gray matter volume recovery in treatment-seeking cocaine-addicted individuals: a longitudinal study: PFC recovery after reduced use. Addiction Biology. 2016;22:1391–1401. [PubMed: 27126701]
21. King SG, Gaudreault P-O, Malaker P, Kim J, Alia-Klein N, Xu J, et al. Microstructural Impairments in a Topologically Distinct Prefrontal-Habenular Connection in Cocaine Addiction. Neuron. 2022;accepted.
22. First M, Spitzer R, Gibbon M, J W. Structured clinical interview for DSM-IV axis I disorders - Patient edition (SCID-I/P, Version 2.0). Biometrics Research Department New York State Psychiatric Institute; 1996.
23. Sheehan DV, Lecrubier Y, Sheehan KH, Amorim P, Janavs J, Weiller E, et al. The Mini-International Neuropsychiatric Interview (M.I.N.I.): The development and validation of a structured diagnostic psychiatric interview for DSM-IV and ICD-10. Journal of Clinical Psychiatry. 1998;59:22–33.
24. McLellan AT, Kushner H, Metzger D, Peters R, Smith I, Grissom G, et al. The fifth edition of the addiction severity index. Journal of Substance Abuse Treatment. 1992;9:199–213. [PubMed: 1334156]

25. Kampman KM, Volpicelli JR, Mcginnis DE, Alterman AI, Weinrieb RM, D'Angelo L, et al. Reliability and validity of the cocaine selective severity assessment. Addictive Behaviors. 1998;23:449–461. [PubMed: 9698974]
26. Gossop M The development of a short opiate withdrawal scale (SOWS). Addictive Behaviors. 1990;15:487–490. [PubMed: 2248123]
27. Tiffany ST, Singleton E, Haertzen CA, Henningfield JE. The development of a cocaine craving questionnaire. Drug and Alcohol Dependence. 1993;34:19–28. [PubMed: 8174499]
28. Heinz AJ, Epstein DH, Schroeder JR, Singleton EG, Heishman SJ, Preston KL. Heroin and cocaine craving and use during treatment: Measurement validation and potential relationships. Journal of Substance Abuse Treatment. 2006;31:355–364. [PubMed: 17084789]
29. Gossop M, Griffiths P, Powis B, Strang J. Severity of dependence and route of administration of heroin, cocaine and amphetamines. British Journal of Addiction. 1992;87:1527–1536. [PubMed: 1458032]
30. Heatherton TF, Kozlowski LT, Frecker RC, Fagerström KO. The Fagerström Test for Nicotine Dependence: a revision of the Fagerström Tolerance Questionnaire. Br J Addict. 1991;86:1119–1127. [PubMed: 1932883]
31. Wilkinson GS Wide Range Achievement Test 3. Wilmington, DE: Wide Range, Inc; 1993.
32. Wechsler D Wechsler Abbreviated Scale of Intelligence. San Antonio, TX: Psychological Corporation; 1999.
33. Beck AT, Steer RA, Garbin MG. Psychometric properties of the Beck Depression Inventory: Twenty-five years of evaluation. Clinical Psychology Review. 1988;8:77–100.
34. Beck AT, Epstein N, Brown G, Steer RA. An inventory for measuring clinical anxiety: Psychometric properties. Journal of Consulting and Clinical Psychology. 1988;56:893–897. [PubMed: 3204199]
35. Milenkovic S, Dragovic M. Modification of the Edinburgh Handedness Inventory: A replication study. Laterality. 2013;18:340–348. [PubMed: 22747439]
36. Tournier JD, Smith R, Raffelt D, Tabbara R, Dhollander T, Pietsch M, et al. MRtrix3: A fast, flexible and open software framework for medical image processing and visualisation. NeuroImage. 2019;202:116137. [PubMed: 31473352]
37. Smith SM, Jenkinson M, Woolrich MW, Beckmann CF, Behrens TEJ, Johansen-Berg H, et al. Advances in functional and structural MR image analysis and implementation as FSL. NeuroImage. 2004;23:208–219.
38. Cordero-Grande L, Christiaens D, Hutter J, Price AN, Hajnal JV. Complex diffusion-weighted image estimation via matrix recovery under general noise models. NeuroImage. 2019;200:391–404. [PubMed: 31226495]
39. Andersson JLR, Sotiropoulos SN. An integrated approach to correction for off-resonance effects and subject movement in diffusion MR imaging. NeuroImage. 2016;125:1063–1078. [PubMed: 26481672]
40. Andersson JLR, Sotiropoulos SN. An integrated approach to correction for off-resonance effects and subject movement in diffusion MR imaging. NeuroImage. 2016;125:1063–1078. [PubMed: 26481672]
41. Smith SM, Jenkinson M, Johansen-Berg H, Rueckert D, Nichols TE, Mackay CE, et al. Tract-based spatial statistics: voxelwise analysis of multi-subject diffusion data. NeuroImage. 2006;31:1487–1505. [PubMed: 16624579]
42. Smith SM, Nichols TE. Threshold-free cluster enhancement: Addressing problems of smoothing, threshold dependence and localisation in cluster inference. NeuroImage. 2009;44:83–98. [PubMed: 18501637]
43. Mori S, Oishi K, Jiang H, Jiang L, Li X, Akhter K, et al. Stereotaxic white matter atlas based on diffusion tensor imaging in an ICBM template. NeuroImage. 2008;40:570–582. [PubMed: 18255316]
44. Menzler K, Belke M, Wehrmann E, Krakow K, Lengler U, Jansen A, et al. Men and women are different: Diffusion tensor imaging reveals sexual dimorphism in the microstructure of the thalamus, corpus callosum and cingulum. NeuroImage. 2011;54:2557–2562. [PubMed: 21087671]

45. Takao H, Hayashi N, Ohtomo K. Sex dimorphism in the white matter: Fractional anisotropy and brain size. Journal of Magnetic Resonance Imaging. 2014;39:917–923. [PubMed: 24123288]
46. Powell JL, Parkes L, Kemp GJ, Sluming V, Barrick TR, García-Fiñana M. The effect of sex and handedness on white matter anisotropy: A diffusion tensor magnetic resonance imaging study. Neuroscience. 2012;207:227–242. [PubMed: 22274289]
47. Rippon G, Jordan-Young R, Kaiser A, Fine C. Recommendations for sex/gender neuroimaging research: key principles and implications for research design, analysis, and interpretation. Frontiers in Human Neuroscience. 2014;8:1–13. [PubMed: 24474914]
48. Roalf DR, Quarmley M, Elliott MA, Satterthwaite TD, Vandekar SN, Ruparel K, et al. The impact of quality assurance assessment on diffusion tensor imaging outcomes in a large-scale population-based cohort. NeuroImage. 2016;125:903–919. [PubMed: 26520775]
49. Fortier CB, Leritz EC, Salat DH, Lindemer E, Maksimovskiy AL, Shepel J, et al. Widespread Effects of Alcohol on White Matter Microstructure. Alcohol Clin Exp Res. 2014;38:2925–2933. [PubMed: 25406797]
50. Lin F, Wu G, Zhu L, Lei H. Heavy smokers show abnormal microstructural integrity in the anterior corpus callosum: A diffusion tensor imaging study with tract-based spatial statistics. Drug and Alcohol Dependence. 2013;129:82–87. [PubMed: 23062873]
51. Baeza-Loya S, Velasquez KM, Molfese DL, Viswanath H, Curtis KN, Thompson-Lake DGY, et al. Anterior cingulum white matter is altered in tobacco smokers: Anterior Cingulum White Matter in Tobacco Smokers. Am J Addict. 2016;25:210–214. [PubMed: 27001211]
52. Savjani RR, Velasquez KM, Thompson-Lake DGY, Baldwin PR, Eagleman DM, De La Garza R II, et al. Characterizing white matter changes in cigarette smokers via diffusion tensor imaging. Drug and Alcohol Dependence. 2014;145:134–142. [PubMed: 25457737]
53. Jansen JM, van Holst RJ, van den Brink W, Veltman DJ, Caan MWA, Goudriaan AE. Brain function during cognitive flexibility and white matter integrity in alcohol-dependent patients, problematic drinkers and healthy controls: Brain function and WM in AUD. Addiction Biology. 2015;20:979–989. [PubMed: 25477246]
54. Ashtari M, Cervellione K, Cottone J, Ardekani BA, Kumra S. Diffusion abnormalities in adolescents and young adults with a history of heavy cannabis use. Journal of Psychiatric Research. 2009;43:189–204. [PubMed: 19111160]
55. Gruber SA, Silveri MM, Dahlgren MK, Yurgelun-Todd D. Why so impulsive? White matter alterations are associated with impulsivity in chronic marijuana smokers. Experimental and Clinical Psychopharmacology. 2011;19:231–242. [PubMed: 21480730]
56. Assaf Y, Pasternak O. Diffusion Tensor Imaging (DTI)-based White Matter Mapping in Brain Research: A Review. J Mol Neurosci. 2008;34:51–61. [PubMed: 18157658]
57. Budde MD, Kim JH, Liang H-F, Schmidt RE, Russell JH, Cross AH, et al. Toward accurate diagnosis of white matter pathology using diffusion tensor imaging. Magn Reson Med. 2007;57:688–695. [PubMed: 17390365]
58. Horsfield MA, Jones DK. Applications of diffusion-weighted and diffusion tensor MRI to white matter diseases - a review. NMR Biomed. 2002;15:570–577. [PubMed: 12489103]
59. Le Bihan D Looking into the functional architecture of the brain with diffusion MRI. Nat Rev Neurosci. 2003;4:469–480. [PubMed: 12778119]
60. Pierpaoli C, Basser PJ. Toward a quantitative assessment of diffusion anisotropy. Magn Reson Med. 1996;36:893–906. [PubMed: 8946355]
61. Pierpaoli C, Barnett A, Pajevic S, Chen R, Penix L, Virta A, et al. Water Diffusion Changes in Wallerian Degeneration and Their Dependence on White Matter Architecture. NeuroImage. 2001;13:1174–1185. [PubMed: 11352623]
62. Wheeler-Kingshott CAM, Cercignani M. About “axial” and “radial” diffusivities. Magn Reson Med. 2009;61:1255–1260. [PubMed: 19253405]
63. Moore EE, Hohman TJ, Badami FS, Pechman KR, Osborn KE, Acosta LMY, et al. Neurofilament relates to white matter microstructure in older adults. Neurobiology of Aging. 2018;70:233–241. [PubMed: 30036759]

64. Winklewski PJ, Sabisz A, Naumczyk P, Jodzio K, Szurowska E, Szarmach A. Understanding the Physiopathology Behind Axial and Radial Diffusivity Changes—What Do We Know? Front Neurol. 2018;9:92. [PubMed: 29535676]

65. Narayana PA, Herrera JJ, Bockhorst KH, Esparza-Coss E, Xia Y, Steinberg JL, et al. Chronic cocaine administration causes extensive white matter damage in brain: Diffusion tensor imaging and immunohistochemistry studies. Psychiatry Research: Neuroimaging. 2014;221:220–230.

66. Scholz J, Tomassini V, Johansen-Berg H. Individual Differences in White Matter Microstructure in the Healthy Brain. Diffusion MRI: From Quantitative Measurement to In-vivo Neuroanatomy, . 2nd ed. Elsevier; 2014. p. 301–316.

67. Jeurissen B, Leemans A, Tournier J-D, Jones DK, Sijbers J. Investigating the prevalence of complex fiber configurations in white matter tissue with diffusion magnetic resonance imaging: Prevalence of Multifiber Voxels in WM. Hum Brain Mapp. 2013;34:2747–2766. [PubMed: 22611035]

68. Chamberland M, Raven EP, Genc S, Duffy K, Descoteaux M, Parker GD, et al. Dimensionality reduction of diffusion MRI measures for improved tractometry of the human brain. NeuroImage. 2019;200:89–100. [PubMed: 31228638]

69. Kousik SM, Napier TC, Carvey PM. The Effects of Psychostimulant Drugs on Blood Brain Barrier Function and Neuroinflammation. Front Pharmacol. 2012;3.

70. Bachtell RK, Jones JD, Heinzerling KG, Beardsley PM, Comer SD. Glial and neuroinflammatory targets for treating substance use disorders. Drug and Alcohol Dependence. 2017;180:156–170. [PubMed: 28892721]

71. Gonçalves J, Baptista S, Silva AP. Psychostimulants and brain dysfunction: A review of the relevant neurotoxic effects. Neuropharmacology. 2014;87:135–149. [PubMed: 24440369]

72. Pereira RB, Andrade PB, Valentão P. A Comprehensive View of the Neurotoxicity Mechanisms of Cocaine and Ethanol. Neurotox Res. 2015;28:253–267. [PubMed: 26105693]

73. Belachew S, Rogister B, Rigo JM, Malgrange B, Moonen G. Neurotransmitter-mediated regulation of CNS myelination: a review. Acta Neurol Belg. 1999;99:21–31. [PubMed: 10218089]

74. Zhang Y, Zhang H, Wang L, Jiang W, Xu H, Xiao L, et al. Quetiapine enhances oligodendrocyte regeneration and myelin repair after cuprizone-induced demyelination. Schizophrenia Research. 2012;138:8–17. [PubMed: 22555017]

75. Ersland KM, Skrede S, Stansberg C, Steen VM. Subchronic olanzapine exposure leads to increased expression of myelination-related genes in rat fronto-medial cortex. Transl Psychiatry. 2017;7:1262. [PubMed: 29187753]

76. Rothman RB, Baumann MH. Monoamine transporters and psychostimulant drugs. European Journal of Pharmacology. 2003;479:23–40. [PubMed: 14612135]

77. Johnson S, North R. Opioids excite dopamine neurons by hyperpolarization of local interneurons. J Neurosci. 1992;12:483–488. [PubMed: 1346804]

78. Smith HR, Beveridge TJR, Nader MA, Porrino LJ. Regionally-specific alterations in myelin proteins in nonhuman primate white matter following prolonged cocaine self-administration. Drug and Alcohol Dependence. 2014;137:143–147. [PubMed: 24529965]

79. Lassmann H, van Horssen J. Oxidative stress and its impact on neurons and glia in multiple sclerosis lesions. Biochimica et Biophysica Acta (BBA) - Molecular Basis of Disease. 2016;1862:506–510. [PubMed: 26432481]

80. Cunha-Oliveira T, Rego AC, Oliveira CR. Cellular and molecular mechanisms involved in the neurotoxicity of opioid and psychostimulant drugs. Brain Research Reviews. 2008;58:192–208. [PubMed: 18440072]

81. Cadet JL, Bisagno V, Milroy CM. Neuropathology of substance use disorders. Acta Neuropathol. 2014;127:91–107. [PubMed: 24292887]

82. Sajja RK, Rahman S, Cucullo L. Drugs of abuse and blood-brain barrier endothelial dysfunction: A focus on the role of oxidative stress. J Cereb Blood Flow Metab. 2016;36:539–554. [PubMed: 26661236]

83. Kaufman MJ Cocaine-Induced Cerebral Vasoconstriction Detected in Humans With Magnetic Resonance Angiography. JAMA. 1998;279:376. [PubMed: 9459471]

84. Buttner A Neuropathological Alterations in Cocaine Abuse. CMC. 2012;19:5597–5600.

85. Büttner A, Rohrmoser K, Mall G, Penning R, Weis S. Widespread axonal damage in the brain of drug abusers as evidenced by accumulation of β-amyloid precursor protein (β-APP): an immunohistochemical investigation. Addiction. 2006;101:1339–1346. [PubMed: 16911734]

86. Andersen SN, Skullerud K. Hypoxic/ischaemic brain damage, especially pallidal lesions, in heroin addicts. Forensic Science International. 1999;102:51–59. [PubMed: 10423852]

87. Wang Y, Li W, Li Q, Yang W, Zhu J, Wang W. White matter impairment in heroin addicts undergoing methadone maintenance treatment and prolonged abstinence: A preliminary DTI study. Neuroscience Letters. 2011;494:49–53. [PubMed: 21362458]

88. Li W, Li Q, Wang Y, Zhu J, Ye J, Yan X, et al. Methadone-induced Damage to White Matter Integrity in Methadone Maintenance Patients: A Longitudinal Self-control DTI Study. Sci Rep. 2016;6:19662. [PubMed: 26794650]

89. Zhuang W, Tang Y, Zhong N, Jiang H, Du J, Wang J, et al. Persistent Microstructural Deficits of Internal Capsule in One-Year Abstinent Male Methamphetamine Users: a Longitudinal Diffusion Tensor Imaging Study. J Neuroimmune Pharmacol. 2016;11:523–530. [PubMed: 27115910]

90. Kaag AM, van Wingen GA, Caan MWA, Homberg JR, van den Brink W, Reneman L. White matter alterations in cocaine users are negatively related to the number of additionally (ab)used substances: White matter and cocaine use. Addiction Biology. 2017;22:1048–1056. [PubMed: 26860848]

91. Ritchie SJ, Cox SR, Shen X, Lombardo MV, Reus LM, Alloza C, et al. Sex Differences in the Adult Human Brain: Evidence from 5216 UK Biobank Participants. Cerebral Cortex. 2018;28:2959–2975. [PubMed: 29771288]

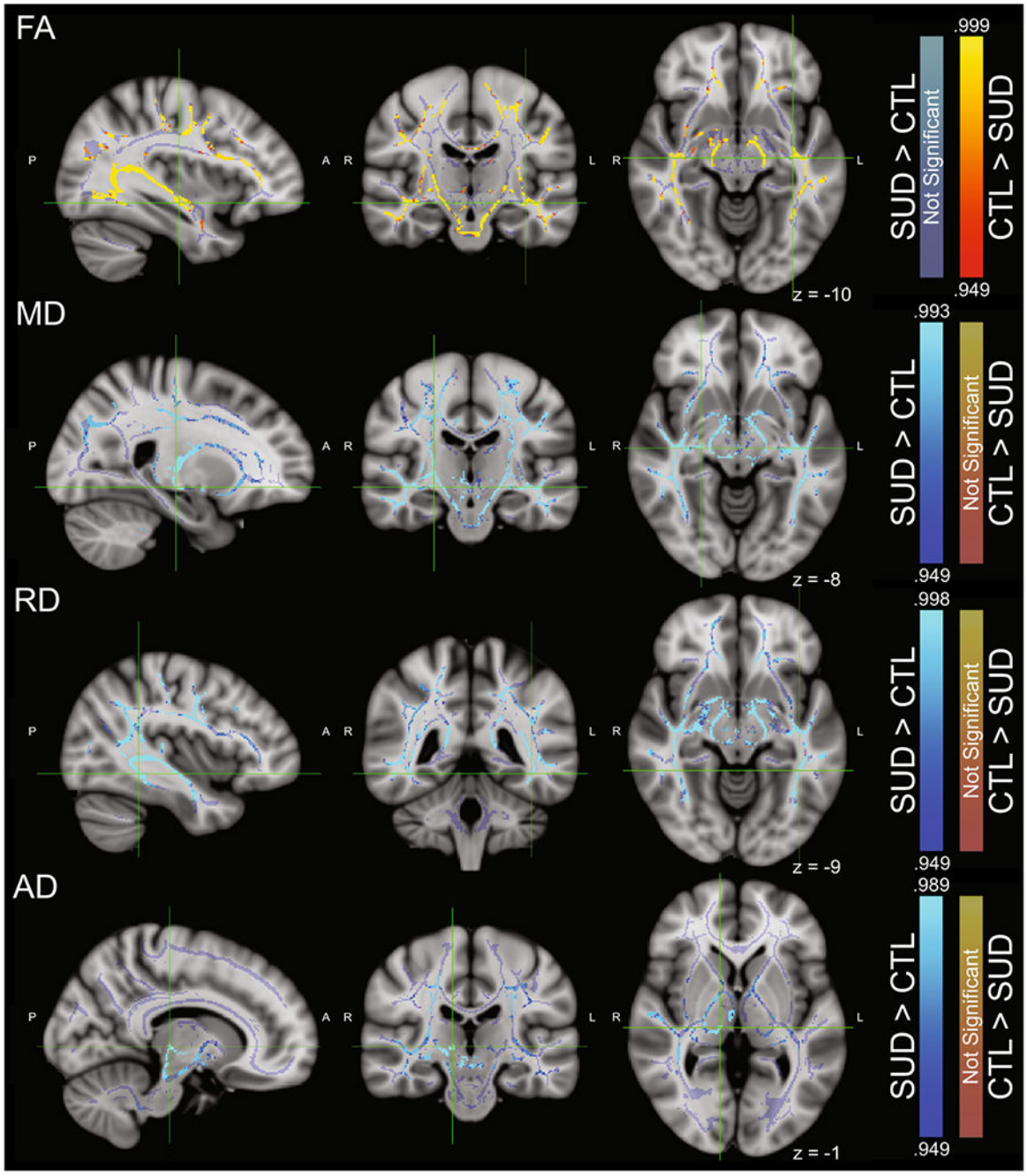

Figure 1:

Whole-brain differences between healthy controls (CTL) and individuals with substance use disorder (SUD).

This figure represents group difference maps thresholded at significant voxels (1-p > .949 TFCE corrected). Maps of significant voxels are overlaid on a study-specific white matter skeleton (in light purple) and the MNI152 template. Brain maps are represented according to the radiological convention (the right hemisphere is displayed on the left side). Warm colors represent voxels where CTL show higher intensity than individuals with SUD whereas cool

colors show the opposite. The coordinates of the peak intensity (i.e., the highest p-value) for each image is depicted by a green location cursor.

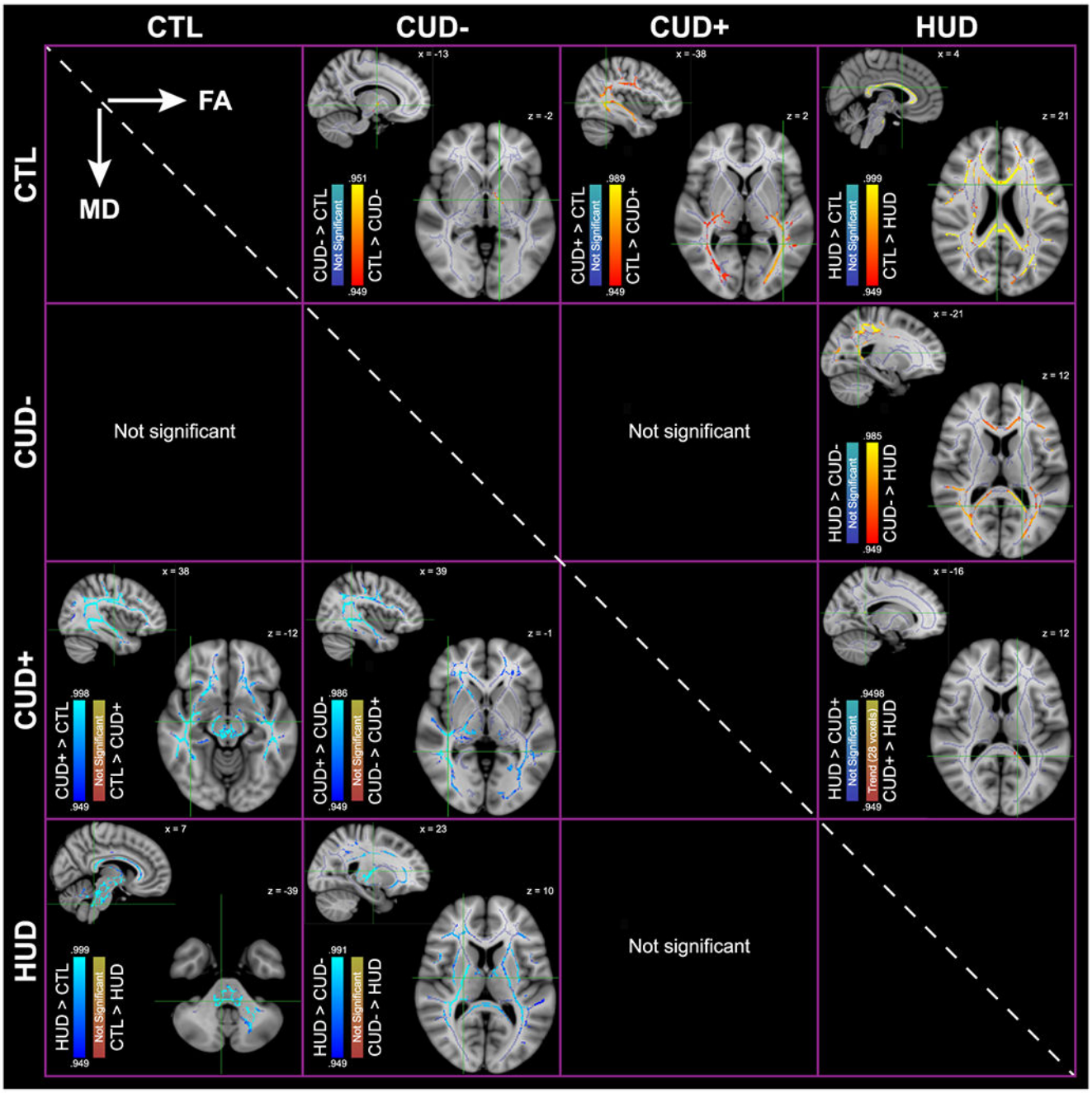

Figure 2:

Group-specific whole-brain differences of fractional anisotropy (FA) and mean diffusivities (MD).

This figure represents thresholded maps of significant voxels (1-p > .949 TFCE corrected) between all study groups [healthy controls (CTL), abstinent cocaine users (CUD−), current cocaine users (CUD+), and individuals with heroin use disorder (HUD)] on FA and MD. Legends show the direction of the effects for each case. Maps of significant voxels are overlaid on a study-specific white matter skeleton (in light purple) and the MNI152

template. Brain maps are represented according to the radiological convention (the right hemisphere is displayed on the left side). The coordinates of the peak intensity (i.e., the highest p-value) for each image is depicted by a green location cursor.

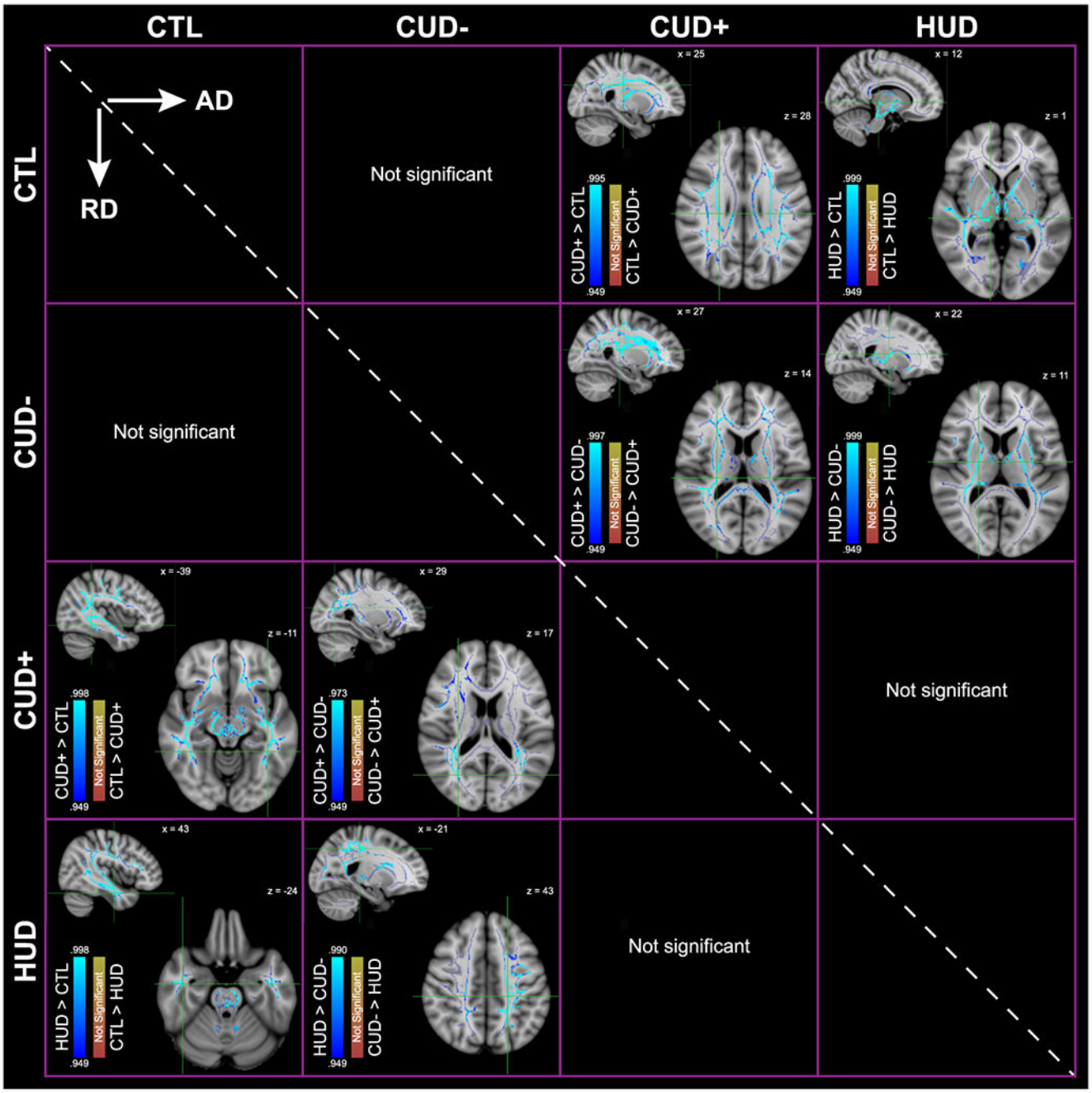

Figure 3:

Group-specific whole-brain differences of axial (AD) and radial diffusivities (RD). This figure represents thresholded maps of significant voxels (1-p > .949 TFCE corrected) between all study groups [healthy controls (CTL), abstinent cocaine users (CUD−), current cocaine users (CUD+), and individuals with heroin use disorder (HUD)] on AD and RD. Legends show the direction of the effects for each case. Maps of significant voxels are overlaid on a study-specific white matter skeleton (in light purple) and the MNI152 template. Brain maps are represented according to the radiological convention (the right

hemisphere is displayed on the left side). The coordinates of the peak intensity (i.e., the highest p-value) for each image is depicted by a green location cursor.

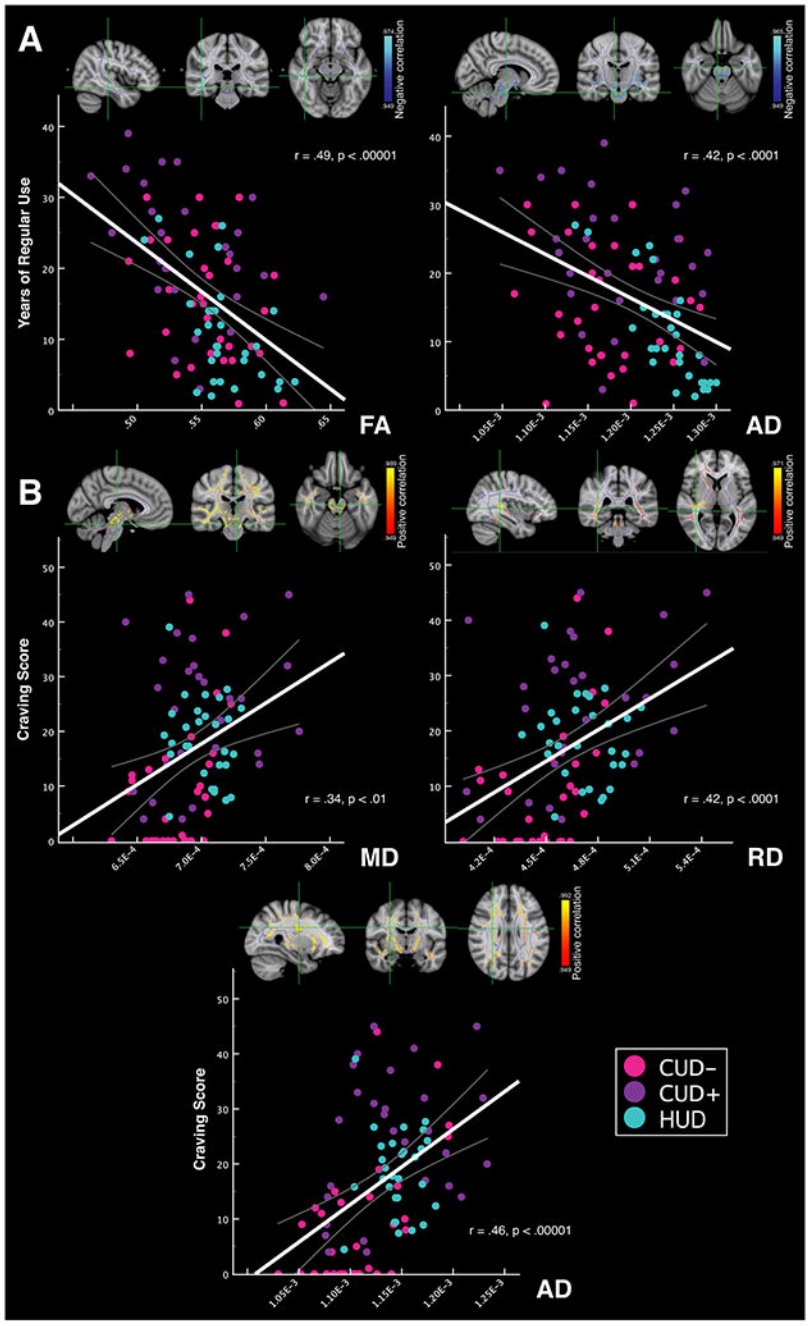

Figure 4:

Significant whole-brain voxelwise correlations between drug use variables and white matter (WM) diffusion metrics in individuals with SUD.

This figure shows scatterplots of the correlations between years of regular use (A) and craving scores (B) with the averaged extracted diffusivity values across significant (1-p > .949 TFCE corrected) voxels for the fractional anisotropy (FA), mean (MD), radial (RD), and axial diffusivities (AD) in abstinent cocaine users (CUD−, pink), current cocaine users (CUD+, purple), and individuals with heroin use disorder (HUD, cyan). The regression line

(white) represents the correlation across the entire SUD group. Maps of significant voxels are overlaid on a study-specific white matter skeleton (in light purple) and the MNI152 template. Brain maps are represented according to the radiological convention (the right hemisphere is displayed on the left side). The coordinates of the peak intensity (i.e., the highest p-value) for each image is depicted by a green location cursor.

Table 1 –

Demographic characteristics, neuropsychological measures, and drug-of-choice (DOC) use variables of the study sample

	Healthy Controls	Abstinent cocaine users	Current cocaine users	Heroin use disorder	Statistical analyses	
	CTL, N = 58	CUD−, N = 32	CUD+, N = 28	HUD, N = 30	Test	*p* value
Demographics						
Age (years)	39.3 ± 8.6[a]	47.3 ± 7.9[b]	47.7 ± 6.5[b]	40.3 ± 9.0[a]	$F_{(3,147)}$ = 11.0	**p = .000**
Gender (men/women)	37 / 21	28 / 4	22 / 6	24 / 6	χ^2 = 7.1	p = .068
Education (years)	14.2 ± 2.2[a]	12.3 ± 1.7[b]	12.5 ± 1.9[b]	12.2 ± 2.2[b]	$F_{(3,147)}$ = 9.8	**p = .000**
Race (Black or African-American/White/Other & Mixed)	41[a] / 7[a] / 7	21[a] / 4[a] / 4	26[a] / 0[a] / 1	2[b] / 21[b] / 7	χ^2 = 64.4	**p = .000**
Intracranial volume (liters)	1.65 ± .17	1.72 ± .14	1.65 ± .16	1.67 ± .16	$F_{(3,147)}$ = 1.6	p = .196
Absolute displacement correction (millimeters)	1.3 ± .46	1.5 ± .81	1.4 ± .80	1.0 ± .37	$F_{(3,145)}$ = 2.9	p = .023
Neuropsychological and self-reported tests						
WRAT – Reading Scale (standard score)	100.5 ± 9.6[a]	96.2 ± 11.3	93.3 ± 11.1[b]	92.7 ± 11.4[b]	$F_{(3,147)}$ = 4.9	**p = .003**
WASI – Matrix Reasoning (scaled score)	10.5 ± 2.8	10.8 ± 2.2	9.0 ± 3.2	10.6 ± 2.6	$F_{(3,145)}$ = 2.6	p = .052
Handedness (right/left/ambidextrous)	54 / 3 / 1	26 / 2 / 3	27 / 0 / 1	26 / 4 / 0	χ^2 = 9.8	p = .133
Depression (BDI)	5.2 ± 7.2[a]	7.5 ± 8.0[a]	6.1 ± 6.3[a]	14.0 ± 12.7[b]	$F_{(3,143)}$ = 7.2	**p = .000**
Anxiety (BAI)	2.6 ± 5.6[a]	4.3 ± 7.0[a]	5.0 ± 8.1[a]	11.31 ± 11.4[b]	$F_{(3,141)}$ = 8.0	**p = .000**
DOC (and other drug) use variables						
Days of alcohol use during past 30 days	1.9 ± 3.1[a]	2.0 ± 4.1[a]	5.0 ± 5.7[b]	.04 ± 0.2[a]	$F_{(3,135)}$ = 8.2	**p = .000**
Cigarette smokers (Current/Past/Never)	10[a] / 8 / 37[a]	19[b] / 9 / 4[b]	27[c] / 1 / 0[b]	30[c] / 0 / 0[b]	χ^2 = 91.4	**p = .000**
Fagerström Test for Nicotine Dependence	1.4 ± 1.6[a]	4.4 ± 2.3[b]	2.4 ± 1.8[a]	3.7 ± 1.6[b]	$F_{(3,80)}$ = 6.6	**p = .000**
Age of first use (years)	--	22.9 ± 6.1	20.6 ± 5.9	24.6 ± 6.6	$F_{(2,88)}$ = 2.6	p = .078
Years of regular use	--	15.5 ± 8.6[a]	22.6 ± 8.9[b]	11.1 ± 7.4[a]	$F_{(2,89)}$ = 14.3	**p = .000**
Period of heaviest use (years)	--	4.3 ± 3.9	7.0 ± 8.2	5.7 ± 7.3	$F_{(2,86)}$ = 1.2	p = .305
Current abstinence (days)	--	538.0 ± 1161.9	2.8 ± 2.8	198.6 ± 265.1	$F_{(2,89)}$ = 4.4	p = .015
Days of DOC use during past 30 days	--	2.3 ± 5.3[a]	12.1 ± 9.1[b]	0.2 ± 0.8[a]	$F_{(2,89)}$ = 32.3	**p = .000**

	Healthy Controls	Abstinent cocaine users	Current cocaine users	Heroin use disorder	Statistical analyses	
	CTL, N = 58	CUD−, N = 32	CUD+, N = 28	HUD, N = 30	Test	*p* value
Severity of Dependence Scale	--	5.6 ± 5.6[a]	4.5 ± 3.6[a]	10.2 ± 3.6[b]	$F_{(2,88)} = 13.5$	**p = .000**
DOC withdrawal symptoms (adjusted score)	--	14.6 ± 11.5	22.8 ± 12.9	14.1 ± 14.2	$F_{(2,89)} = 4.1$	p = .019
DOC subjective craving (adjusted score)	--	8.8 ± 11.5[a]	24.5 ± 12.4[b]	16.9 ± 12.5[b]	$F_{(2,88)} = 16.5$	**p = .000**

Notes: Data expressed as frequencies or means ± standard deviation (SD). WRAT: Wide Range Achievement Test; WASI: Wechsler Abbreviated Scale Intelligence. In order to correct for multiple comparisons, p values were considered significant at $p < 0.005$ (0.05/11 statistical tests) for the demographics/neuropsychological tests and $p < 0.005$ (0.05/11 statistical tests) for the DOC use variables. Post hoc analyses were carried out with Tukey HSD tests for F statistics and with Bonferroni-corrected adjusted residuals for chi-square tests. Superscripts refer to the significant between-group post hoc contrasts, e.g., the same superscript means that groups did not differ. Withdrawal symptoms were calculated with two different scales for both DOC, i.e., the Cocaine Selective Severity Scale and the Subjective Opiate Withdrawal Scale. Subjective cravings were also assessed in a drug-specific way, i.e., the 5-items cocaine craving scale and Heroin Craving Questionnaire. HUD withdrawal and craving scores were converted to the CUD scales to allow for statistical comparisons. For 10 of the Table 1 variables (demographics, Neuropsychological tests, and self-reported drug use variables), up to three participants in each group had missing data.

Table 2 -

Clustered white matter differences between healthy control subjects (CTL), abstinent (CUD−) and current individuals with cocaine (CUD+), and individuals with heroin use disorder (HUD)

					Commissural							Projection								As
	Clusters	Effects	Voxels	Max 1-*p*	GCC	BCC	SCC	TAP	ACR	SCR	PCR	ALIC	PLIC	RLIC	PTR	CP	SLF	SFO	UF	SS
CTL vs. CUD−																				
FA	c1	CTL > CUD−	138	.951								**L**	**L**							
CTL vs. CUD+																				
FA	c1	CTL > CUD+	8 257	.989							L			**L**	**L**		**L**			L
	c2	CTL > CUD+	3 194	.967									R	**R**	**R**	**R**				**R**
	c3	CTL > CUD+	230	.951	**X**	**X**														
	c4	CTL > CUD+	141	.950																
MD	c1	CUD+ > CTL	64 700	.998		X				L							R			
RD	c1	CUD+ > CTL	57 248	.998		X			B								B			
AD	c1	CUD+ > CTL	28 427	.995		X			R	B	B		B	R			B			
	c2	CUD+ > CTL	188	.949	**X**	**X**			**L**											
CTL vs. HUD																				
FA	c1	CTL > HUD	44 568	.999	X	**X**	X		B						L					
MD	c1	HUD > CTL	55 718	.999		X	X		L	L							B			
	c2	HUD > CTL	278	.957																
RD	c1	HUD > CTL	58 188	.998	X	X	X		L											
AD	c1	HUD > CTL	26 459	.999			X			B			B	B			B			
CUD+ vs. CUD−																				
MD	c1	CUD+ > CUD−	27 194	.986		X			R	R	R		R	R	R		**R**			R
	c2	CUD+ > CUD−	19 245	.981		X			L	**L**	L						**L**			

					Commissural				Projection											As
	Clusters	**Effects**	**Voxels**	**Max 1-*p***	**GCC**	**BCC**	**SCC**	**TAP**	**ACR**	**SCR**	**PCR**	**ALIC**	**PLIC**	**RLIC**	**PTR**	**CP**	**SLF**	**SFO**	**UF**	**SS**
RD	c1	CUD+ > CUD−	13 282	.973		X			R	R	R		**R**	R			**R**			R
	c2	CUD+ > CUD−	7 314	.973						**L**	**L**		**L**	L			**L**			L
AD	c1	CUD+ > CUD−	39 682	.997		X	X		B	B			B				R			
HUD vs. CUD−																				
FA	c1	CUD− > HUD	9 277	.980	**X**	**X**	**X**				**B**			L	**B**					
	c2	CUD− > HUD	5 155	.985						**L**							**L**			
	c3	CUD− > HUD	193	.953						**L**							**L**			
	c4	CUD− > HUD	125	.950					**R**											
MD	c1	HUD > CUD−	39 510	.991		X	X			B			R				R			
RD	c1	HUD > CUD−	35 172	.990	X	X	X		R	L					L					
	c2	HUD > CUD−	235	.953																
AD	c1	HUD > CUD−	24 285	.999					L	B		L	B	B			R			R
HUD vs. CUD+																				
FA	c1	CUD+ > HUD	28	.949			**X**													

Notes: Threshold-Free Cluster Enhancement (TFCE) correction was used for all analyses to account for multiple comparisons. Significance for group differences was considered at 1-p > .949. The right part of the table represents the averaged probabilities of all significant voxels from a cluster to overlap with the “JHU ICBM-DTI-81 White-Matter Atlas” labels. Specific regions are divided into types of fibers (commissural, projection, association, and tracts in the brainstem). Localization of significant regions was identified with an overlap threshold of 2%. “X” is used for non-lateralized regions. “L/R/B” correspond to Left / Right / Bilateral regions. Bold and underline cases represent overlap probabilities >5%.

Acronyms (in the presented order): [Commissural fibers] GCC: genu of corpus callosum, BCC: body of corpus callosum, SCC: splenium of corpus callosum, TAP: tapetum. [Projection fibers] ACR: anterior corona radiata, SCR: superior corona radiata, PCR: posterior corona radiata, ALIC: anterior limb of internal capsule, PLIC: posterior limb of internal capsule, RLIC: retrolenticular part of internal capsule, PTR: posterior thalamic radiation, CP: cerebral peduncle. [Association fibers] SLF: superior longitudinal fasciculus, SFO: superior fronto-occipital fasciculus, UF:

uncinate fasciculus, SS: sagittal stratum, EC: external capsule, CgC: cingulum in the cingulate cortex, CgH: cingulum in the hippocampal region, FX / ST: fornix/stria terminalis. [Tracts in the brainstem] CST: corticospinal tracts, ML: medial lemniscus, ICP: inferior cerebellar peduncle, MCP: middle cerebellar peduncle, SCP: superior cerebellar peduncle.